Atomic Force Microscopy Measurements of Adsorbed Polyelectrolyte Layers. 1. Dynamics of Forces and Friction

ARTICLE *in* LANGMUIR · APRIL 2003

Impact Factor: 4.46 · DOI: 10.1021/la026570p

3 AUTHORS, INCLUDING:

Adam Armitage Feiler
KTH Royal Institute of Technology
25 PUBLICATIONS **903** CITATIONS
SEE PROFILE

Mark W Rutland
KTH Royal Institute of Technology
148 PUBLICATIONS **3,564** CITATIONS
SEE PROFILE

Atomic Force Microscopy Measurements of Adsorbed Polyelectrolyte Layers. 1. Dynamics of Forces and Friction

Adam Feiler, Mark A. Plunkett, and Mark W. Rutland*

Department of Chemistry, Surface Chemistry, Royal Institute of Technology, SE-100 44 Stockholm, Sweden, and The Institute for Surface Chemistry, P.O. Box 5607, SE-11486 Stockholm, Sweden

Received September 17, 2002. In Final Form: March 5, 2003

The measurement of surface forces and friction between silica substrates bearing adsorbed layers acrylamide−1% [3-(2-methylpropionamide)propyl]trimethylammonium chloride (AM-MAPTAC) was examined using atomic force microscopy. The cationic polymer had a large molecular weight (900 000) and a very low charge density (1% MAPTAC units). The force curves in the presence of adsorbed polyelectrolyte showed a very long range repulsive interaction and large deformation on compression typical of electrosteric interactions and consistent with the expected adsorption profile. There was also a strong dependence on the scan rate with increased repulsion during approach and increased attraction during separation as the scan rate increased. The hysteresis was attributed entirely to a hydrodynamic interaction induced by the polyelectrolyte. At slow enough scan rates, the hysteresis between approach and retract curves was absent. The friction force measurements were sensitive to both applied load and scan rate. With increasing applied load, a critical load was apparent, above which the friction force increased. Upon decrease of the load, the friction force remained higher than that before the yield point, suggesting a metastable deformation of the polymer layer. In addition, the friction coefficient increased with increasing scan rate. At low scan rates the friction coefficient was lower than the bare surfaces, whereas at high scan rates the friction coefficient was significantly larger that obtained than for the bare surfaces. Subsequent force curves taken after friction measurements confirm that a permanent change in the polyelectrolyte layer had occurred. The magnitude of the repulsive interaction was reduced to about half of its original force.

Introduction

Cationic polyelectrolytes have a range of uses in many industrial applications such as water treatment, mineral separation, papermaking, food science, and medical science.[1−7] The underlying connection in all the applications is modifying colloidal interaction forces by the presence (or absence) of an adsorbed polymeric layer. Adsorption of macromolecules to solid surfaces in solution is accomplished by the ability of macromolecule to anchor with several segments at once. The affinity of the polymer for the surface can be increased by the introduction of charges on the polymer of opposite sign to that of the surface. By control of quantities such as concentration, charge density, and chain length, polyelectrolytes can be tailored to provide a host of functions. For example a highly charged polymer at high concentration promotes colloidal stability by providing a repulsive electrostatic and steric barrier to particle aggregation. Conversely, at low concentrations, the same polyelectrolyte may be used to increase flocculation by mutual adsorption on adjacent particles by "bridging".[8]

The importance in understanding the polyelectrolyte adsorption mechanisms is obvious. However, possibly even more important for a quantitative understanding of the role of adsorbed polyelectrolyte is the ability to be able to directly measure the interaction forces in situ. Over the past decades there have been many reports of the role of factors such as polymer type, solvency, and molecular weight on interaction forces using the surface force apparatus (SFA) (see for example refs 9−12). However the great majority of these have been concerned with neutral polymers. Studies of polyelectrolytes are much less extensive.[13−15]

In this paper the modification of surface forces and friction between silica surfaces bearing an adsorbed layer of cationic polyelectrolyte has been investigated using atomic force microscopy (AFM). The use of the colloidal probe technique[16,17] is ideally suited to the study of surface and friction forces at the molecular level. In this paper a random copolymer consisting of 99% acrylamide (AM) and 1% [3-(2-methylpropionamide)propyl]trimethylammonium chloride (MAPTAC) with a large molecular mass (900 000

* To whom the correspondence should be addressed. E-mail: mark.rutland@surfchem.kth.se.

(1) Hesselink, T. T. *J. Colloid Interface Sci.* **1977**, *60*, 448−465.
(2) Survey of polyelectrolyte coagulant use in the United States. *J. Am. Water Works Assoc.* **1982**, *74*, 600−608.
(3) Wagberg, L.; Kolar, K. *Ber. Bunsen-Ges. Phys. Chem.* **1996**, *100*, 984−993.
(4) Kulicke, W. M.; Kniewske, R.; Hörl, H. H. *Angew. Makromol. Chem.* **1980**, *87*, 195.
(5) *Industrial Gums*: *Polysacherides and their Derivatives*; Academic: San Diego, CA, 1993.
(6) Williams, H. R.; Fletcher, D. S.; Elbert, E. E.; Lin, T. Y. *Biochim. Biophys. Acta* **1983**, *757*, 69.
(7) Fant, C.; Sott, K.; Elwing, H.; Höök, F. *Biofouling* **2000**, *16*, 119−132.
(8) Israelachvili, J. *Intermolecular & Surface Forces*, 6th ed.; Academic Press: San Diego, CA, 1997.
(9) Luckham, P. F.; Klein, J. *J. Chem. Soc., Faraday Trans.* **1990**, *86*, 1363−1368.
(10) Klein, J.; Kumacheva, E.; Perahia, D.; Mahalu, D.; Warburg, S. *Faraday Discuss.* **1994**, *98*, 173−188.
(11) Israelachvili, J.; Tirrell, M.; Klein, J.; Almog, Y. *Macromolecules* **1984**, *17*, 204−209.
(12) Marra, J.; Hair, M. L. *Macromolecules* **1987**, *21*, 2349−2355.
(13) Dahlgren Mats, A. G.; Aasa, W.; Blomberg, E.; Claesson, P. M.; Sjoestroem, L.; Aakesson, T.; Jonsson, B. *J. Phys. Chem.* **1993**, *97*, 11769−11775.
(14) Claesson P M.; Fielden M L.; Dedinaite A *J. Phys. Chem. B* **1998**, *102*, 1270−1278.
(15) Claesson, P.; Dedinaite, A.; Blomberg, E.; Sergeyev, V. G. *Ber. Bunsen-Ges. Phys. Chem.* **1996**, *100*, 1008−1013.
(16) Ducker, W. A.; Senden, T. J.; Pashely, R. M. *Langmuir* **1992**, *8*, 1831.
(17) Ducker, W. A.; Senden, T. J.; Pashely, R. M. *Nature* **1991**, *353*, 239.

10.1021/la026570p CCC: $25.00
Published on Web 04/18/2003

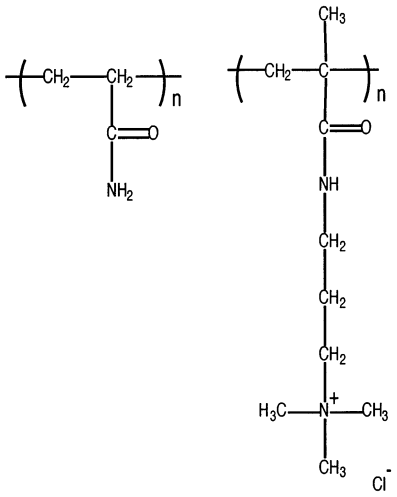

Figure 1. Schematic representation of the monomers AM (left) and MAPTAC (right).

g/mol) has been used. Previous studies have shown that this low charged polyelectrolyte adsorbs at negatively charged surfaces in a diffuse extended conformation. It was therefore of interest to observe how the expected long-range electrosteric layer would affect both the normal and frictional forces and if the adsorbed layer remains robust to mechanical action. In a subsequent paper[18] we examine the effect of changing both the charge density of the polyelectrolyte and underlying substrate in which both of these changes increase the affinity of the adsorption.

Materials and Methods

Materials. Analytical grade KBr was used throughout. Milli-Q water was used in all solutions. Polished silicon wafers, thermally oxidized to produce a SiO_2 layer of 170 nm, were kindly provided by Dr. Stefan Klintström (University of Linköping, Sweden). The silica substrates were cut to into 1 cm squares, cleaned by thorough rinsing in water and then ethanol, and then plasma treated (PDG-32G plasma cleaner, Harrick Scientific Corp., USA) on medium setting for 1 min.

The experiments were all conducted in a background electrolyte of 10^{-4} M KBr in Milli-Q water. The polymer used in the study was a 900 000 g/mol molecular mass random copolymer consisting of 99% acrylamide (AM) and 1% [3-(2-methylpropionamide)-propyl]trimethylammonium chloride (MAPTAC). The AM is an uncharged monomer while the MAPTAC is positively charged leading to a charge density of 1% of monomers. The polyelectrolyte was synthesized and kindly provided by the Laboratorie de Physico-Chemie Macromoleculaire (Paris). Schematics of both monomers are shown in Figure 1.

Methods. *AFM Instrument.* A Nanoscope IIIa Multimode atomic force microscope (Digital Instruments, Santa Barbara, CA) equipped with a fluid cell was used. Solutions were introduced into the cell via syringe and Teflon tubing. The solutions were sucked into the cell using a syringe attached at the *outlet* port via tubing and a freshly cleaned piece of tubing attached to the inlet port placed below the meniscus of the solution contained in a glass vial (30 mL). This procedure was adopted because it was found to be effective at preventing air bubbles from being introduced into the cell, which is often seen to occur in the normal method of injecting the solutions via syringe.

Colloidal Probe Preparation. The process of functionalizing AFM cantilevers by the attachment of spherical micrometer-sized particles is now common practice.[16,17] In this work, tipless rectangular cantilevers (CSC12, MikroMasch, Estonia) were used. Silica beads ($R \approx 10\ \mu$m) (Duke Scientific Corp., USA) were attached to the cantilevers using a very small amount of quick-setting two-part epoxy resin (Araldite). Two etched tungsten wires attached to a micromanipulator arm were used to position first a tiny quantity of glue and then a glass bead at the tip of the cantilever under microscopic control (Nikon, Japan). The cantilever was left for at least 12 h to allow the glue to fully cure. The functionalized cantilever comprises the so-called colloid probe. The radius of the attached sphere was determined by an optical microscope. Immediately prior to measurement the colloid probe was cleaned by rinsing in Milli-Q water and then ethanol, then blown dry under nitrogen, and finally plasma treated (PDG-32G plasma cleaner, Harrick Scientific) on medium setting for 1 min.

Spring Constant Calculations. The cantilevers' normal spring constant were determined from the change in resonant frequency upon attachment of a series of tungsten spheres to the end of the cantilever.[19,20] A minium of three tungsten spheres per cantilever was used. The normal spring constants were determined to be 4.2 ± 0.6 N/m. A linear correlation was observed between the resonant frequency of the unloaded cantilever and the calculated normal spring constant for 20 cantilevers from the same batch. This indicated a consistent material property of the cantilevers with the slight variation in spring constant being attributed to a difference in the thickness most likely from the thickness of the reflective coating.

Quantitative measurements of the friction force were possible once the torsional spring constant of the AFM cantilever is known. The cantilever torsional spring constant was determined according to two recently developed calibration protocols. With the method of Feiler et al.,[21] a glass fiber attached orthogonally to the end of the cantilever provided torque as the cantilever was bought into contact with a flat silicon substrate. The second calibration procedure was a method proposed by Rutland[22] in which a second cantilever with integrated tip glued on the lower surface acts as a pivot which twists the cantilever as it is brought into contact with the pivot. The procedure was simplified by pressing the cantilever at three contact points only, one in the center line of the cantilever (where the probe was to be mounted) and one at either side as close as possible to the widths edge. Since the width of the cantilever could be determined accurately using optical microscopy, this avoided using the piezo movement to measure the distance. Both calibration methods were in quantitative agreement and yielded an average value of $(3.2 \pm 0.1) \times 10^{-8}$ N m/rad for 10 cantilevers. The torsional spring constant varied between 2.7 and 4.1 $\times 10^{-8}$ N m/rad, and there was a linear correlation between the normal and torsional spring constant.

A calibration constant of the photodiode for lateral force measurement was obtained using the method of Meurk and Larson[22] in which the lateral voltage signal was recorded as the laser beam moved laterally across the photodiode using the stepper motor to tilt a mirrored substrate.

Friction Measurements. The friction force was calculated from so-called friction force loops by taking the average friction force between the forward and reverse scan directions as the substrate was moved under the colloid probe. In all measurements a scan size of 5 μm was used. The friction force was measured as a function of increasing then decreasing load. Also for some measurements the applied load was kept constant as the scan rate was varied.

Results

To discern the effects of the adsorbed polyelectrolyte on both the normal and frictional forces, it was first necessary to characterize these forces for the bare substrates. In Figure 2, we show the force−distance data for the interaction between two silica surfaces in 10^{-4} M KBr solution conducted at 0.2 Hz. The force is normalized by

(18) Plunkett, M. A.; Feiler, A.; Rutland, M. W. *Langmuir* **2003**, *19*, 4180−4187.

(19) Sader, J. E. *Rev. Sci. Instrum.* **1995**, *66*, 4583−4587.

(20) Cleveland, J. P.; Manne, S.; Bocek, D.; Hansma, P. K. *Rev. Sci. Instrum.* **1993**, *65*, 403−405.

(21) Feiler, A.; Attard, P.; Larson, I. *Rev. Sci. Instrum.* **2000**, *71*, 2746−2750.

(22) Bogdanovic, G.; Meurk, A.; Rutland, M. W. *Colloids Surf., B* **2000**, *19*, 397−405.

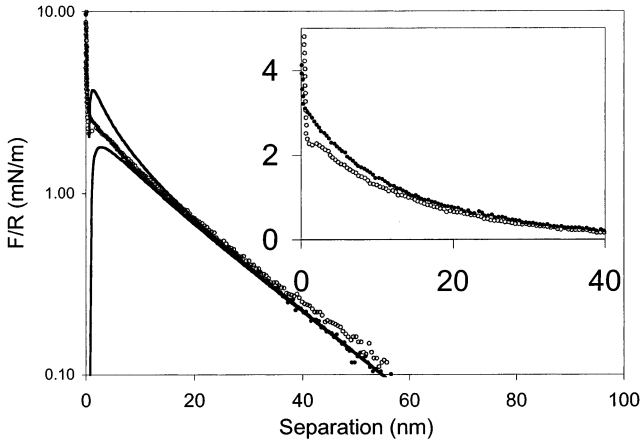

Figure 2. Force−distance curves (semilog plot) on approach (solid symbols) and retract (open symbols) for a silica sphere ($R = 10\ \mu$m) and a flat silica surface in 10^{-4} M KBr. The main figure is for a rate of 0.2 Hz, with theoretical force curves generated according to DLVO theory (under constant charge (top) and constant potential (bottom) boundary conditions with a diffuse layer potential of −85 mV and Debye length 17.62 nm). A Hamaker constant of 0.8×10^{-20} J was used in the calculations. The inset is experimental results for a rate of 14 Hz (plotted as a linear plot for clarity).

the sphere radius in accordance with the Derjuaguin approximation[23] such that

$$F/R = 2\pi G$$

where F is the interaction force, R is the radius of the sphere, and G is the free energy of interaction. Also shown in the figure are predictions of the double layer interaction forces based upon DLVO theory.[8] The theoretical force curves were generated using the AFM Analysis program of Ip et al.[24] by assuming a symmetric interaction. As can been seen in the semilog plot, there is good agreement between the measured force curves and theory with the data lying between the constant charge and constant potential boundary conditions. A diffuse layer potential of −85 mV was used in the calculation, and this is in good agreement with other measurements on similar silica systems.[25]

The inset in Figure 2 shows a force−distance curve for the same system run at the maximum frequency of 14 Hz. As can be seen, at this rate, at small separations (below 25 nm) there is a slight difference between approach and retract force profile, whereas at the slower frequency of 0.2 Hz (main figure) the approach and retract curves are concomitant. The difference in the two data curves in the inset is a dynamic effect and can be accounted for by hydrodynamic considerations.[26] This inset is included to demonstrate that the effect of hydrodynamics is small and yet measurable at high scan rates in colloidal probe measurements.

The frictional force as a function of increasing load for the silica−silica system is shown in Figure 3. There is a linear relation between the load and the frictional force, with a friction coefficient of 0.59. The friction force upon decreasing load followed the same trend. It was found however that over time (1 h), the system underwent some changes. In the friction traces, this led to a decrease in the

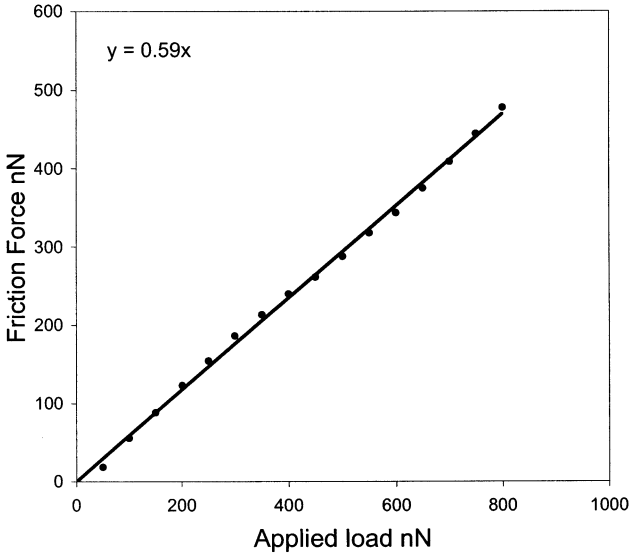

Figure 3. Friction as a function of load for the interaction of two silica surfaces in 10^{-4} M KBr at 1 Hz rate. The linear trendline is fitted to estimate a friction coefficient of 0.59.

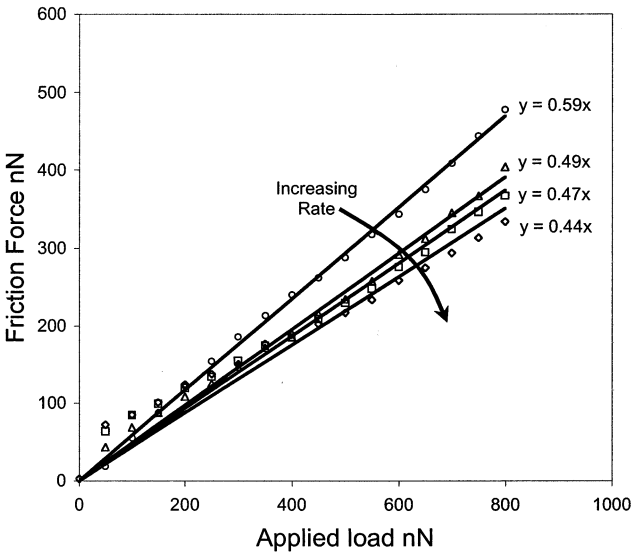

Figure 4. Friction as a function of load for silica substrates at different loads. The straight line fits are used to obtain a friction coefficient. The different rates are, from top to bottom, 1 Hz (circles), 2 Hz (triangles), 5 Hz (squares), and 10 Hz (diamonds). The friction coefficients decrease with increasing shear rate.

friction coefficient (down to 0.3 over 1 h) and a nonzero friction force at negative loads (due to the adhesion). Both the increase in adhesion and decrease in the friction coefficient may be attributed to smoothing of surface asperities by the mechanical action. In addition, the effect of scan rate on the friction force was investigated and, as seen in Figure 4, the friction coefficient decreases with increasing scan rate. There is approximately 25% decrease in the friction coefficient with a 10-fold increase in rate (1−10 Hz).

The adsorption of AM-MAPTAC-1% to the silica surfaces was achieved from a bulk solution of 20 ppm of the polyelectrolyte in 10^{-4} M KBr. The system was allowed to equilibrate for 1 h, and the bulk polymer was kept in solution for the entire course of the experiments. Normal force measurements were then taken prior to conducting frictional measurements. These results are shown in Figure 5 for a range of different approach speeds. For

(23) Derjaguin, B. V. *Kolloid-Z.* **1934**, *69*, 155−164.
(24) Ip l; Chan, D. Y. C. *Venters In*, 2 ed.; Department of Mathematics, University of Melbourne, Australia.: Melbourne, 1994.
(25) Hartley, P. G.; Larson, I.; Scales, P. J. *Langmuir* **1997**, *13*, 2207−2214.
(26) Chan, D. Y. C.; Horn, R. G. *J. Chem. Phys.* **1985**, *83*, 5311−5324.

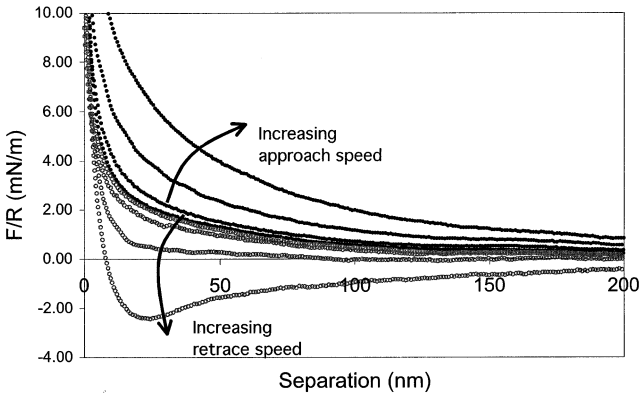

Figure 5. Force−distance curves for AM-MAPTAC-1% adsorbed onto silica surfaces. The solid symbols represent forces on approach and open symbols represent forces on retract. The different runs are for various rates, increasing away from a nonhysteretic slow rate curve with increasing rate as indicated by the arrows. The rates (starting from the center and moving out) are 0.1, 1, 5, and 14 Hz.

runs of 0.1 Hz or slower (1 μm piezo expansion), the approach and retract curves overlay each other and show a long-range purely repulsive interaction (out to 250 nm). At rates faster than 0.1 Hz, a hysteresis between approach and retract became evident, increasing with the increase in frequency of the run.

As can be seen in Figure 5, the repulsive force on approach became larger, while the retract force became more negative, and, at sufficiently high frequency, entered into the attractive regime. Note that even when an attraction was seen, the curves were smooth with no evidence of a jump out. The force curves were fully reproducible course of the measurements indicating that the force-measuring process did not affect the polymer layer.

After the normal force curves were measured, the frictional forces were investigated. For all the friction force curves, there was a marked difference between increasing and decreasing loads (see Figure 6). In Figure 6a, it can be seen that there is load-induced change in the system at between 400 and 600 nN. This change leads to a rapid increase in the frictional force, from a low load linear regime up to a second regime with an increased friction coefficient. Upon decrease of load (Figure 6b), the friction force tends to a more linear function of load and there is a clear hysteresis between the loading and unloading cycles. The effect of scan rate on the friction forces is also shown in Figure 6. Here it is seen that frictional force increases with rate. Note that this is in opposition to the effect seen for the bare substrates. The load-activated change is evident in Figure 6a, regardless of rate. However, there seems to be a significant difference between the 1 Hz and faster runs, the 1 Hz case resulting in significantly reduced friction. For all the scan rates, the friction force tends to be linear with decreasing load, Figure 6b. The friction coefficient has clearly increased with scan rate as indicated in the figure. It is important to note that after the fastest scan rate of 10 Hz, the scan rate of 1 Hz was repeated and the same frictional behavior was observed as before the scan rate series was performed. This fact clearly eliminates wear/damage/reconstruction of the surface as a possible explanation and confirms that the observation is truly rate dependent.

After conducting the friction experiments, the normal forces were again measured to determine if there had been any changes to the polymer layer. This was important since there was both a small time effect, and a significant load-induced increase in the friction. As can be seen in Figure 7, there is a significant difference between the normal force curves made prior to the friction studies and those taken subsequently. Of particular note is the much reduced range of the steric repulsion after friction measurements. In addition, the retract data showed a significant difference, indicating both an adhesion and a much longer range than on approach. It was also noted that the retract indicated steps rather than a smooth monotonic change in magnitude. These altered force curves were found not to change appreciably over the course of half an hour, which was the longest duration forces were measured after the friction, indicating that the polymer layers had adopted some type of shear-induced quasi-equilibrium structure.

Discussion

The force and friction data for the bare silica case are shown in order to characterize the substrate and to indicate any changes to the system after addition of polyelectrolyte. The force curves show that the silica layers have a surface charge of roughly 85 mV/m^2 and that the interaction between the surfaces can be described purely by DLVO theory. The presence of a jump in on approach is not always seen for silica interactions in electrolyte. Measurements using measurement and analysis if surface interaction forces (MASIF), for example,[27] display entirely repulsive behavior, with the approach and separation curves being entirely superimposable. The short-range repulsion in that case is generally attributed to a hydration repulsion and can be removed, for example, by the addition of calcium ions. In the case of the MASIF though, glass surfaces are generally used which are unlikely to have identical surface properties to the silica surfaces used here.

The classical (Amontons) linear relationship of friction and load is also usually observed between inorganic substrates with repulsive surface forces and is reminiscent of a multiasperity contact.[28,29] The fact that there were changes in the frictional behavior with time tends to suggest a slight smoothing of the surface or possibly even a marginal furrowing. However, on addition of the polyelectrolyte, a new contact position was used, and thus silica−silica contact is unlikely to have occurred. Thus the most relevant measurements to compare with are those made early in the silica−silica experiment as the surface at that time is most representative of the substrate underlying the polyelectrolyte layer.

The decreasing friction with increasing rate is interesting. From the Stribeck curve,[29] decreasing friction with increasing rate suggests this system is in the mixed lubrication region. This is the region in which the friction moves from a regime where the asperities dominate the friction (boundary friction) to a region in which there is a thick film between the surfaces and thus the asperity contact is negligible. At even higher rates (or viscosities or pressures) the Stribeck curve suggests a change into the elastohydrodynamic and hydrodynamic region, and thus we would then expect an increase in friction with rate.

The hysteresis between the approach and retract curves (Figure 5) after polyelectrolyte addition was shown to have increased with scan rate. Plotted in Figure 8 are both the nonhysteretic 0.1 Hz case and the force curve taken at a

(27) Poptoshev, E.; Claesson, P. M. *Langmuir* **2002**, *18*, 1184−1189.
(28) McClelland, G. M. *Adhesion and friction*; Springer: Berlin, 1989; Vol. 17.
(29) Meyer, E.; Overney, R. M.; Dransfield, K.; Gyalog, T. *Nanoscience: Friction and rheology on the nanometer scale*; World Scientific Publishing: Singapore, 1998.

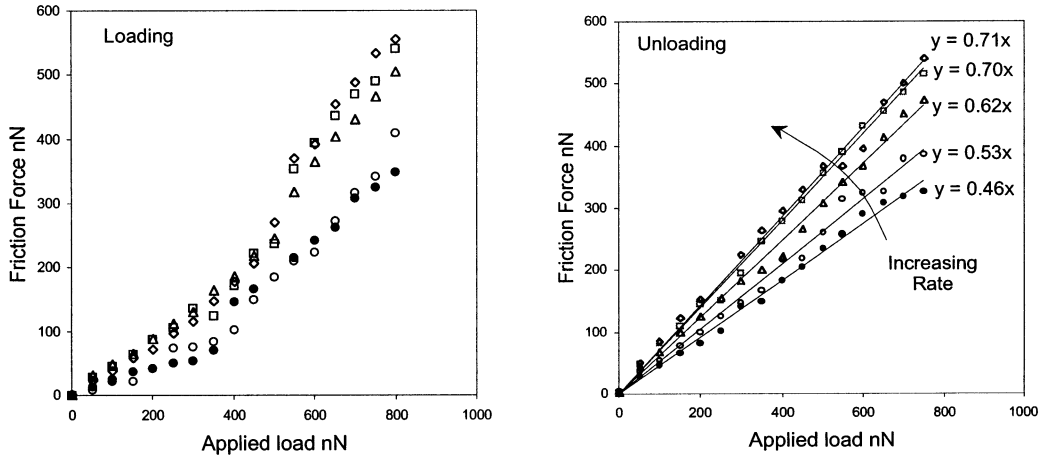

Figure 6. Friction as a function of scan rate during (a) loading and (b) unloading between AM-MAPTAC-1% coated surfaces. The rates were conducted in the following order: 1 Hz (open circles), 2 Hz (open triangles), 5 Hz (open diamond), 10 Hz (open squares), 1 Hz (solid circles).

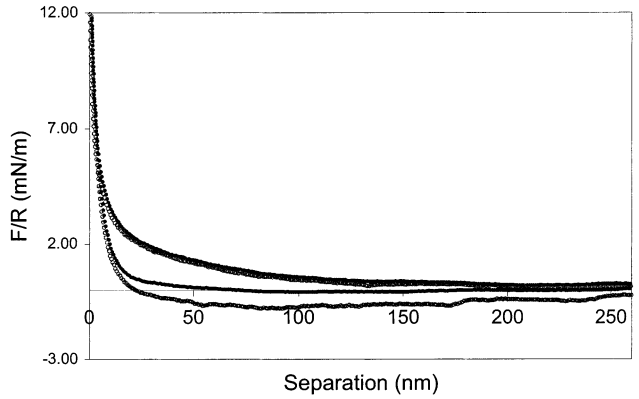

Figure 7. Force−distance curves for AM-MAPTAC-1% adsorbed onto silica substrates. Solid symbols represent data on approach, while open symbols represent data on retraction. The upper two curves are prefriction and the lower two are for postfriction.

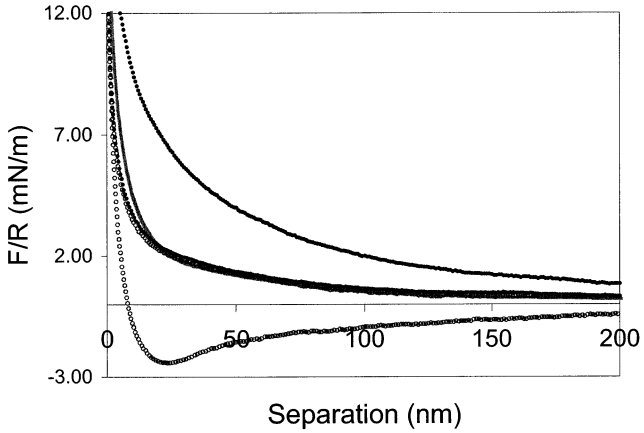

Figure 8. Force−distance curves for AM-MAPTAC-1% on silica. Solid symbols represent data on approach while open symbols represent data on retraction. The middle two sets of data points are for a rate of 0.2 Hz while the outer two sets of data are for 14 Hz rate. The single line which lies almost on top of the middle data points is the average of the approach and retrace curves for the 14 Hz case.

maximum scan rate of 14 Hz (the most hysteretic). Also shown in the figure is the average of the approach and retract curves for the 14 Hz scan rate calculated by averaging the approach and retract data over the scan range. It can be seen that the average of the approach and retract for the 14 Hz run collapses directly onto the 0.1 Hz case. This indicates that for the dynamic hysteresis, the additional force is equal in magnitude but opposite in sign on approach compared to retraction. Dynamic contributions to electrosteric interactions could be due to only a few possibilities. First is a viscoelastic response arising from conformation changes or relaxation effects. Such a mechanism is unlikely to lead to such a "symmetric" effect. By definition it is due to the polymers inability to relax under the time scale of the experiment; thus different responses on loading and unloading would be expected. It is also hard to see how it would cause an attractive regime on separation unless there was a secondary mechanism involving some type interdigitation between the polymers adsorbed on opposing surfaces. The fact that there is no jump-out on retraction (the minimum is smooth and rounded) further suggests that interdiffusion is not the mechanism. Also, the adhesion maximum increases with rate, and since an increase in rate decreases contact time, the trend tends to act in the wrong direction.

A second and more likely mechanism which would manifest as repulsive on approach and attractive on retraction involves hydrodynamic flow of solvent. As seen in the inset of Figure 2 however, the hydrodynamics between two elastic surfaces, such as a silica sphere and wafer, are minimal in both range and magnitude. In the case of adsorbed polyelectrolyte layers however, the flow of solvent within the gap becomes much more complex. For example, the viscosity can no longer be approximated by the bulk solvent since the polymer matrix can greatly reduce the mobility of solvent molecules. In addition, it is not obvious when flow within the polymer starts to occur and it is probable that a Gaussian flow rate distribution across the gap is no longer valid. To attempt to model the hydrodynamics, it is theoretically possible to apply a more complex model with among other things both a variable slipping plane and a variable viscosity; however this is much too complex a proposition for the scope of the current work. As a first approximation however, we have used the hydrodynamics formula of Chan and Horn,[26] and using the separation between the hard walls used in the force calculation, we have varied the viscosity to approximate the difference between the fast and slow runs. In this case the fit cannot be made over the entire separation range, but as a best approximation the input viscosity is roughly 0.2 kg/ms, around 1000 times that of bulk water. This figure is not to be taken too literally but rather as an indication of the resistance imposed by the polymer

network. The value itself is obviously an overestimate due to the fact that because of the polymer, the solvent flow is reduced to only a fraction of the available gap.

A third possibility is that instrument-related dynamic artifacts arise at high rates which lead to spurious forces. At first sight this may seem likely since these would be symmetrical; however, as will be seen in a forthcoming publication[30] such effects are not large enough to cause the magnitude of the effect seen here. Furthermore they appear only when polymer is present.

Figure 7 shows that there was a difference in the normal forces after the friction measurements, which suggests that the friction induces a more collapsed or depleted layer with a lower solvent concentration. This observation is in general irrespective of when the normal force is measured (after little shearing or after the entire friction study is complete). It is thus not due to gradual wear of the layer over the course of the experiment but rather is shear induced, and stable to further shear. It is difficult to say what this shear-induced layer change is due to, but several possibilities exist. First a combing effect may occur with polyelectrolyte being aligned parallel to the scanning direction, resulting in a thinner, less compressible layer with a lower solvent concentration. Second, one or both of the surfaces may be denuded (polymer is removed), leaving a thinner polymer layer on the surface. Third, the shear motion may cause the polymer layer to adopt a denser conformation with a lower solvent concentration, which is stabilized by an entanglement of the loops present. Both the second and third possibilities are supported by the retraction data in Figure 7 which illustrates a small, shallow but long-range minimum. Small steps are also present, and such a force profile is highly reminiscent of either bridging forces (requiring at least some accessible adsorption sites on at least one surface) or alternatively an entanglement between the two polymer layers. It should be kept in mind that the contact point of the probe is always in contact during shear while the lower substrate experiences a much smaller contact time along the 5 μm track. In fact the contact area is around 2 orders of magnitude smaller than the track left on the lower substrate. Thus there is no reason to believe that the layers should be the same on the two surfaces.

Finally, it is noted that the same sort of rate effects are observed after shear in the normal force curves, as in the preshear case. This of course again attributed to hydrodynamic behavior, which is not surprising since the main contribution to the hydrodynamics occurs on regions away from the contact point and at these distances the layers may not even have undergone the shear-induced transition.

The frictional behavior of the layer is very interesting. At low loads a low friction regime is observed on the loading cycle, which is significantly lower than the friction for the bare surfaces (Figure 6a). The layer is relatively thick and contains solvent,[31,32] so this result is not unexpected. The frictional properties are thus more representative of a combined boundary/lubricated regime. At higher loads a threshold is achieved at about 400 nN where the friction behavior undergoes a transition to a more strongly dissipative regime, which suggests that a change occurs in the layer properties. This load is unfortunately too large to register in the normal forces, so we have no supporting evidence. Two possibilities exist, either the layer collapses and expels water or polymer is physically removed from the contact area through some type of plowing mechanism. The fact that the friction behavior at low shear rates is similar to the friction between bare silica argues in favor of polymer removal. This suggests that only when the surfaces are physically out of contact can the material return to the friction path. (The low friction regime is always observed, so the layer re-establishes itself extremely quickly after separation.) If in fact the transition is due to a collapse rather than removal, it may be that the layer is unable to rebound until the surfaces have been separated and water has access to repenetrate the layer. There are thus two distinct changes in the polyelectrolyte films to consider. The first (the depletion of material) is shear induced, occurs immediately, and is permanent over the course of the experiment. The second (the collapse into the friction-load curve) is load induced, stable with respect to unloading, but completely reversible on physical separation of the surfaces.

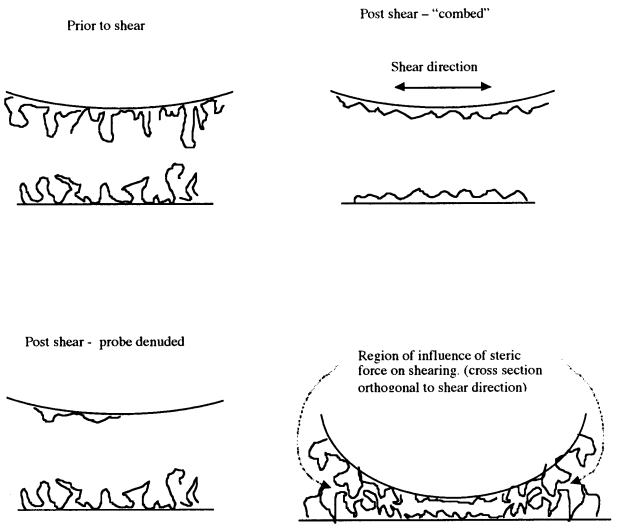

Figure 9. Schematic to illustrate possible polymer conformations and interaction regimes during the force measurements.

Possibly the most interesting aspect of the work is the rate dependence of the friction response which increases almost 50% in going from 1 to 14 Hz. This phenomenon can readily be explained if the dynamics of the normal forces are considered. We know from the normal force measurements (Figure 5) that at high interaction rates there is a viscous resistance which is long ranged. As the surfaces slide over one another, a similar steric interaction is likely to occur in the lateral direction as polymer molecules, particularly those at a distance from the contact point, encounter one another. This is reflected as an extra resistance to shear, i.e., as higher friction. In fact the shear rates for the two types of force measurement are broadly comparable; the friction track was 5 μm and the force curves were 1 μm extensions**.** Thus a 5 Hz force curve corresponds in speed to a 1 Hz friction measurement. Figure 9 shows this effect schematically.

The fact that the shear rate effect on the friction goes in the opposite direction for bare silica (decreasing) to that with the adsorbed polyelectrolyte (increasing with rate) is in itself very interesting. We have already mentioned that interpreting the bare silica interaction via the Stribeck curve suggests that the system is in the mixed solvent regime. Since the polymer leads to an effective increase in the viscosity, it is not surprising that the system could enter a different regime. Hence the interpretation of the data with the Stribeck curve suggest that we have now entered the hydrodynamic regime of

(30) Rutland, M. W.; Tyrell; A. P. Manuscript in preparation.
(31) Plunkett, M. A.; Claesson, P. M.; Rutland, M. W. *Langmuir* **2002**, *18*, 1274.
(32) Plunkett, M. A.; Ernstsson, M.; Claesson, P. M.; Rutland, M. W. Submitted for publication.

friction. Finally, we note that the friction coefficient may be considered to be rather high for the silica−silica case but is consistent with other values obtained for silica using a colloidal probe.[33]

Conclusion

Colloid probe is ideal for studying friction at the nanometer/micrometer scale, particularly for adsorbed layer systems. Having a spherical particle as a probe has several major advantages over AFM with standard tips; for example, the sharp tip may penetrate an adsorbed layer. In addition the adsorption of polymer to a tip will be minimal compared to a much larger surface area of the particle. Colloid probe measurement allows quantitative analysis of normal forces since the Derjaguin approximation can be invoked. The normal forces provide a great deal of information on the nature of the adsorbed layer and its variation in response to the load, time, etc.

It has been shown that adsorbed polyelectrolytes can modify the frictional properties of surfaces and that the frictional response of the layer may exhibit different regimes depending on load and shear rate. In the present study, at low loads adsorbed polyelectrolyte reduced friction due to the high solvent content of the polyelectrolyte film and its relative mobility. At higher loads, increased friction was observed. The explanation for the increased friction is based on observations of the normal forces and the extra dissipative mechanism, which is responsible for both the hysteresis in the normal forces and the increased frictional force at higher rates. This appears to be related to hydrodynamic flow of water through the polyelectrolyte lattice rather than to intrinsic polymer relaxation effects. Further work is underway in this area to confirm this observation.

Acknowledgment. M.P. acknowledges financial support from SSFs CIT program and A.F. acknowledges both the Swedish Research Council (VR) and Unilever Port Sunlight for their support. M.R. also acknowledges the Biofiber Material Centre, BiMaC. We are indebted to Lab. Phys-Chem Macromoleculaire, Paris for the gift of the characterized polyelectrolyte.

LA026570P

(33) Feiler, A. A.; Larson, I.; Jenkins, P.; Attard, P. *Langmuir* **2000**, *16*, 10269.